

Physical effects underlying the transition from primitive to modern cell membranes

Itay Budin and Jack W. Szostak*

*To whom correspondence should be addressed.

Email: szostak@molbio.mgh.harvard.edu

This file includes:

Supporting Online Text

Figures S1-S8

References

Supporting Online Text

Alternate phospholipid synthesis pathways

While our experiments are based on the structure of diacyl phospholipids, archaeal dialkyl phospholipids are quite different (S1). The building blocks of archaeal phospholipid synthesis are pyrophosphate-activated isoprenoids, which are added sequentially to a glycerol phosphate backbone via ether linkages. The ubiquity of isoprenoid synthesis in biology (S3) and the suspected thermophilicity (S2) of the last common ancestor suggest a possible role for archaeal phospholipids early in cellular evolution. However, there are no obvious abiotic pathways for isoprenoid synthesis. Fischer-Tropsch reactions yield straight chain alkanes as their major product (S4), suggesting a metabolic origin (S5, S6) for isoprenoid lipid chains. Nonetheless, the physical phenomena we have described are also likely to apply to branched, dialkyl lipid systems, provided that there is a similar difference in fluidity between monoalkyl and dialkyl membranes.

Calculation of expected growth from desorption rates

Assuming equal adsorption rates for vesicles of different compositions, the partition coefficient (P) of fatty acid monomers between two vesicle populations (A and B) should be inversely

proportional to their corresponding desorption rates: $P = \frac{k_B^{off}}{k_A^{off}}$. This partition coefficient equals

the ratio of the final surface areas (SA) of A and B, so that $P = \frac{1 + \Delta SA_A}{1 + \Delta SA_B}$. Since the growth of

one population must equal the shrinkage of the other, $P = \frac{1 + \Delta SA}{1 - \Delta SA}$ and $\Delta SA = \frac{P - 1}{P + 1}$.

Calculation of free energy of bilayer association from measured desorption rates

The standard free energy of a lipid in a bilayer can be calculated as $\Delta G^\circ = -RT \ln K_{eq}$, where K_{eq} is the equilibrium partition coefficient and is equal to the ratio of on and off rates from the bilayer: $K_{eq} = \frac{k_{on}}{k_{off}}$. If we assume the on rate is constant with varying phospholipid content, K_{eq}

can be expressed in terms of the off rate and equilibrium constants of pure oleic acid:

$K_{eq} = K_{OA} \left(\frac{k_{off}^{OA}}{k_{off}} \right)$. The partition coefficient of oleate can be calculated from its measured critical

aggregation concentration (cac) ($\sim 50 \mu\text{M}$, measured by light scattering of serial dilutions (S7))

via its standard free energy (S8): $\Delta G^\circ_{OA} = RT \ln cac$, where cac is expressed in mole fraction of

solvent; therefore, $K_{OA} = \frac{1}{cac_{OA}}$ and $K_{eq} = \frac{k_{off}^{OA}}{k_{off} * cac_{OA}}$. The standard free energy for oleate given

a measured desorption rate is thus: $\Delta G^\circ = -RT \ln \left(\frac{1}{cac_{OA}} \frac{k_{off}^{OA}}{k_{off}} \right)$, where k_{off} is the measured

desorption rate for oleate in the mixture.

Supplementary Figures

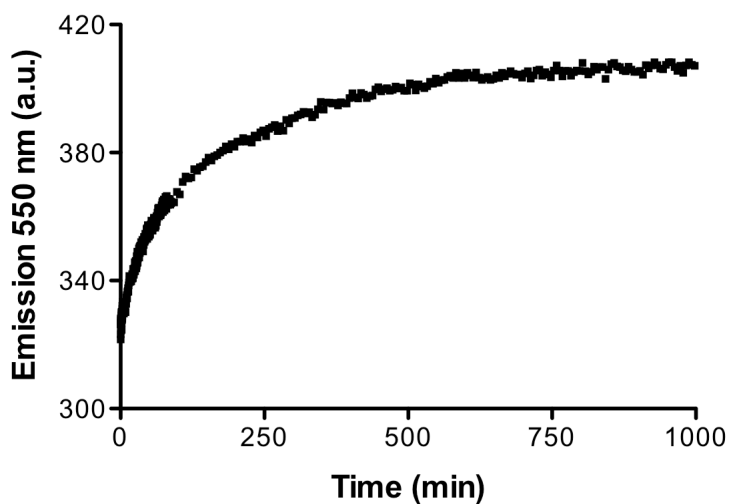


Fig. S1. Bicine permeability is slow in fatty acid-based membranes. 100 nm 2:1:1 DA:DOH:GMD vesicles were prepared in 0.2 M bicine and diluted in a hypertonic solution of 0.5 M bicine. The recovery of encapsulated calcein fluorescence at 550 nm (λ_{ex} 470 nm) within several hours reflects the permeation of bicine across the membrane, returning the vesicles to their initial spherical shape. Other, longer chain-length membrane compositions used in this study exhibited significantly slower bicine permeation.

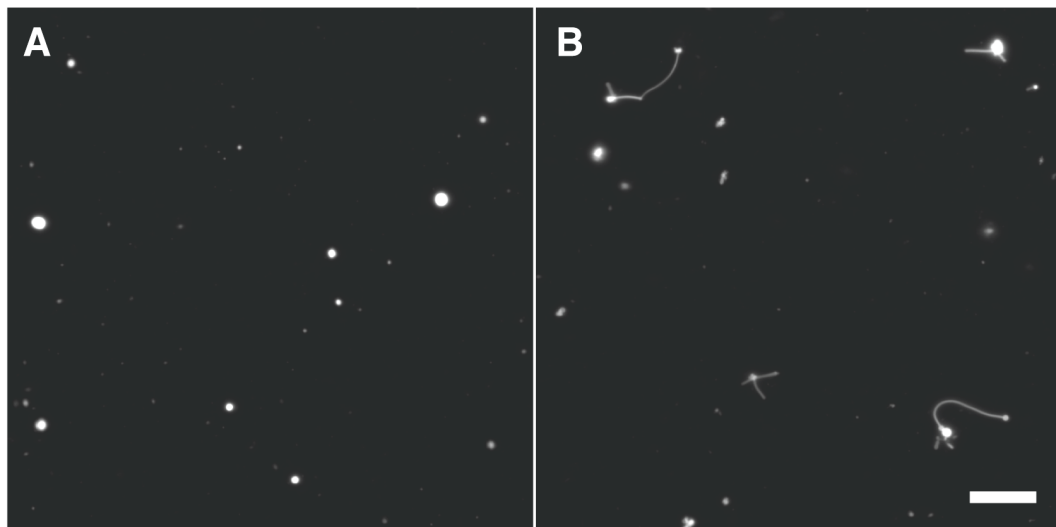


Fig. S2. Phospholipid-driven growth of vesicles composed of short, saturated chain lipids. (A) Large, multilamellar 6:3:1 DA:DOH:DDPA vesicles, labeled with 0.1 mol % Rhodamine DHPE, are initially spherical. (B) Upon mixing with a 5-fold excess of unlabeled 2:1 DA:DOH vesicles, the labeled vesicles grow via the protrusion of thin, tubular tails. Higher amounts of unlabeled vesicles or continual phospholipid synthesis would result in the further vesicle elongation into tubular filaments. Image taken 5 minutes after mixing. Scale bar, 30 μm .

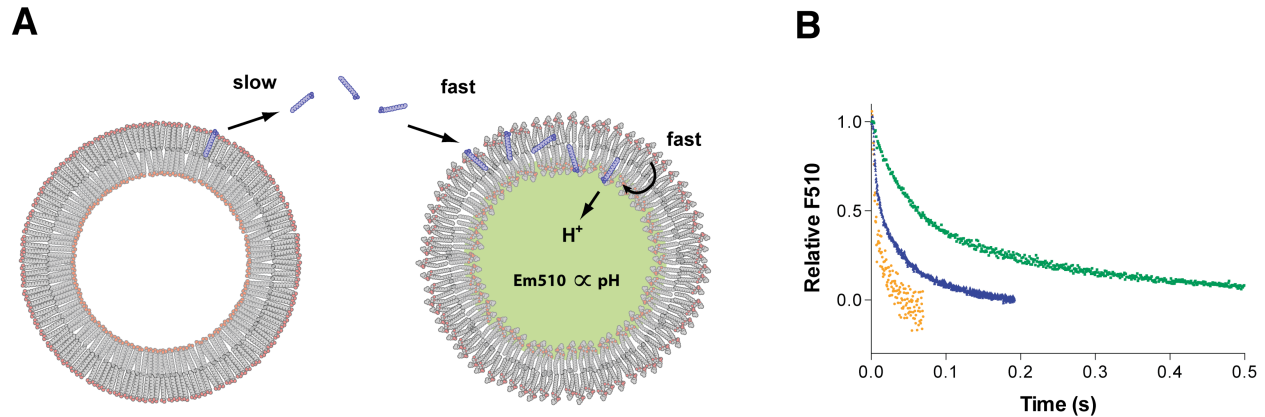


Fig. S3. Measuring fatty acid desorption rates. (A) Schematic for the assay used to measure fatty acid desorption rates. Fatty acid containing vesicles (left) are mixed with phospholipid reporter vesicles (right). The slow desorption of monomers from fatty acid vesicles is followed by their rapid adsorption into phospholipid reporter vesicles, flip-flop, ionization and therefore acidification of the interior of the reporter vesicle. The resulting decrease in fluorescence of the encapsulated pH-sensitive dye HPTS is used to monitor monomer desorption from fatty acid vesicles. (B) Chain length dependence of the rate of monomer desorption from fatty acid membranes. Desorption rate depends on the chain length of the fatty acid: green, oleic acid (C18:1), $k \sim 7.3 \text{ s}^{-1}$; blue, palmitoleic acid (C16:1), $k \sim 34 \text{ s}^{-1}$; orange, myristoleic acid (C14:1), $k \sim 102 \text{ s}^{-1}$. Palmitoleic acid and myristoleic acid were mixed at concentrations of 1 mM and 5 mM, respectively, because of the high critical aggregation concentration of these lipids.

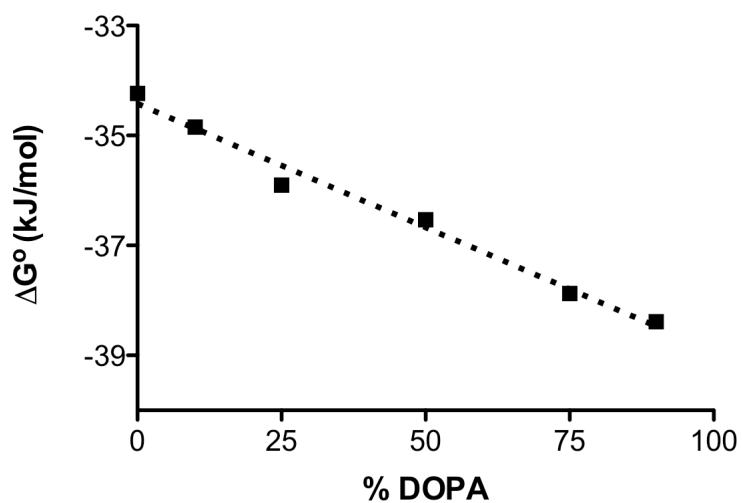


Fig. S4. Free energy of oleate association with mixed oleate/DOPA membranes. Standard free energy of bilayer association relative to solution was calculated (supporting online text) using measured oleate desorption rates (Fig. 3A) and the critical aggregation concentration of oleic acid ($\sim 50 \mu\text{M}$). Dashed line indicates linear regression, $R^2 = 0.99$.

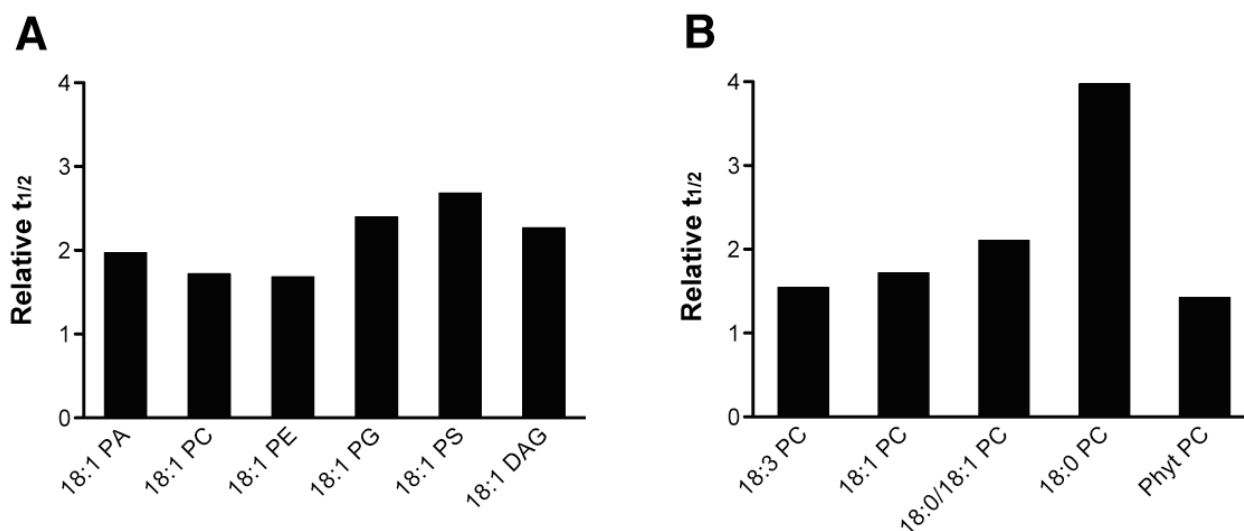


Fig. S5. The effect of phospholipid head group and acyl chains on oleate desorption rates in mixed membranes. (A) The half times of oleate desorption from vesicles containing 25 mol % of the given C18:1 phospholipid, normalized to that in pure oleate membranes. The inhibition of desorption correlates with the hydrogen bonding potential of the phospholipid head groups (e.g. hydroxyls for glycerol, carboxyl, and amine for serine). PA, phosphatidic acid; PC, phosphatidylcholine; PE, phosphatidylethanolamine; PG, phosphatidylglycerol; PS, phosphatidylserine; DAG, diacyl glycerol. (B) The half times of oleate desorption from vesicles containing 25 mol % of the given phosphatidylcholine acyl analogue, normalized to that in pure oleate membranes. Saturated phospholipids, which form ordered bilayers, more strongly inhibited desorption than unsaturated phospholipids, which form disordered bilayers, or branched phospholipids (Phyt PC), which interfere with straight-chain acyl packing. Phyt, di-O-phytanyl, a C20 isoprenoid chain lipid.

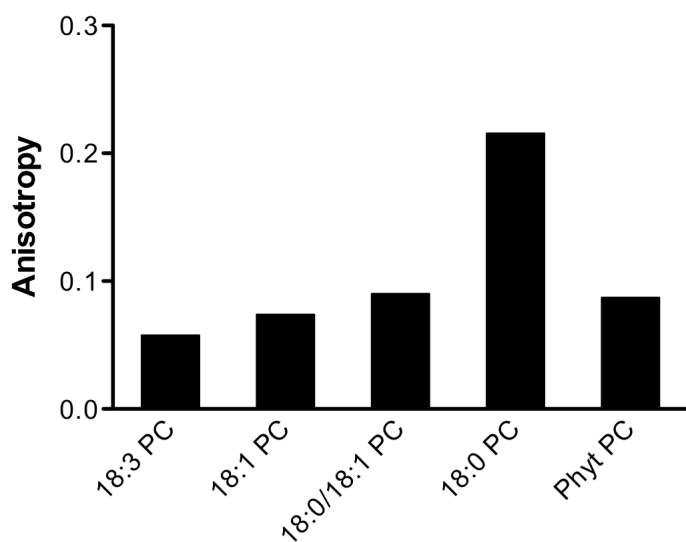


Fig. S6. Anisotropy of mixed membranes containing phospholipids with different acyl chains. The steady-state anisotropy of DPH (0.2 mol %) was measured in oleate vesicles containing 25 mol % of the indicated phosphatidylcholine. Increased anisotropy indicates a more ordered, less fluid bilayer interior, and correlates well with the measured oleate desorption rates from these membranes (Fig. 3A). Phyt, di-O-phytanyl-phosphatidylcholine, a C20 isoprenoid chain lipid.

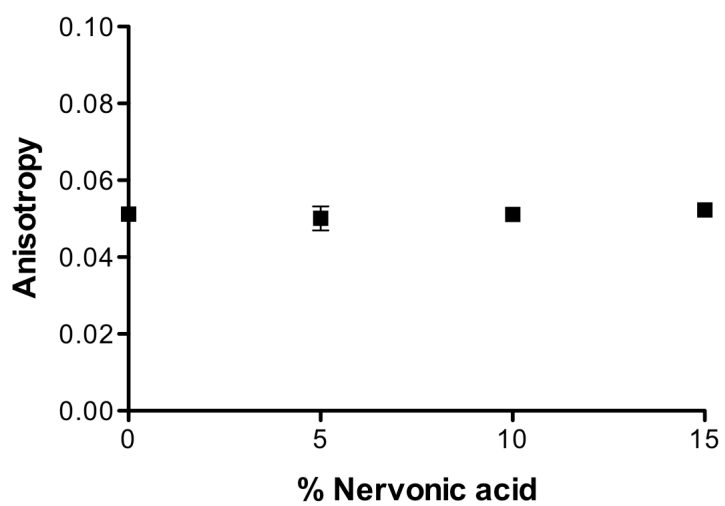


Fig. S7. Steady-state DPH anisotropy of oleate (C18:1) membranes containing nervonic acid (NA) (C24:1). Membrane fluidity is unaffected at 5-15 mol % NA, despite the longer chain length and lower solubility of NA. Error bars indicate S.E.M. (N=3).

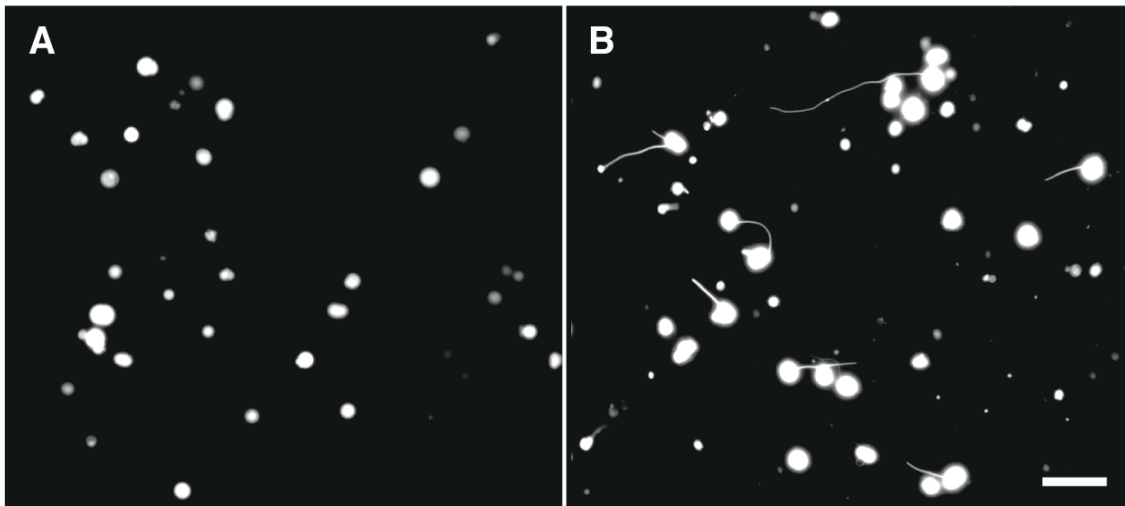


Fig. S8. Growth of phospholipid-enriched mixed vesicles. (A) Large, multilamellar 25:75 oleate:DOPA vesicles, labeled with 0.1 mol % Rhodamine DHPE, are initially spherical. (B) Upon mixing a 10-fold excess of unlabeled 75:25 oleate:DOPA vesicles, the phospholipid-enriched vesicles grow via the protrusion of thin, tubular tails. Growth is limited by the dilution of the initial phospholipid content, but would be continuous in the case of phospholipid-synthesizing protocells. Image taken 5 minutes after mixing. Scale bar, 30 μm .

References

- S1. Koga Y, Morii H (2007) Biosynthesis of ether-type polar lipids in archaea and evolutionary considerations. *Micro. Mol. Bio. Rev.* 71:97-120.
- S2. Benner SA, Ellington AD, Tauer A (1989) Modern metabolism as a palimpsest of the RNA world. *Proc. Natl. Acad. Sci. USA* 86:7054-7058.
- S3. Ciccarelli FD, *et al.* (2006) Toward automatic reconstruction of a highly resolved tree of life. *Science* 311:1283-1287.
- S4. Mccollom TM, Ritter G, Simoneit RT (1999) Lipid synthesis under hydrothermal conditions by Fischer-Tropsch-type reactions. *Orig. Life Evol. Biosph.* 29:153-166.
- S5. Scott IA (1997) How were porphyrins and lipids synthesized in the RNA world? *Tet. Lett.* 38:4961-4964.
- S6. Ryu Y, Scott IA (2003) Efficient one-step synthesis of isoprenoid conjugates of nucleoside 5'-diphosphates. *Org. Lett.* 5:4713-4715.
- S7. Chen IA, Szostak JW (2004) Membrane growth can generate a pH gradient in fatty acid vesicles. *Proc. Natl Acad. Sci. USA* 101:7965-7970.
- S8. Israelachvili JN, Mitchell DJ, Ninham BW (1976) Theory of self-assembly of hydrocarbon amphiphiles into micells and bilayers. *J. Chem. Soc., Faraday Trans. 2* 72:1525-1568.